Editors' Suggestion

Next-to-next-to-leading order QCD corrections to W$b\bar{b}$ production at the LHC

Heribertus Bayu Hartanto,[1,*] Rene Poncelet,[1,†] Andrei Popescu,[1,‡] and Simone Zoia[2,§]

[1]*Cavendish Laboratory, University of Cambridge, Cambridge CB3 0HE, United Kingdom*
[2]*Dipartimento di Fisica and Arnold-Regge Center, Università di Torino, and INFN, Sezione di Torino, Via P. Giuria 1, I-10125 Torino, Italy*

(Received 17 May 2022; accepted 7 September 2022; published 17 October 2022)

We compute theoretical predictions for the production of a W boson in association with a bottom-quark pair at hadron colliders at next-to-next-to-leading order (NNLO) in QCD, including the leptonic decay of the W boson, while treating the bottom quark as massless. This calculation constitutes the very first $2 \to 3$ process with a massive external particle to be studied at such a perturbative order. We derive an analytic expression for the required two-loop five-particle amplitudes in the leading color approximation employing finite-field methods. Numerical results for the cross section and differential distributions are presented for the Large Hadron Collider at $\sqrt{s} = 8$ TeV. We observe an improvement of the perturbative convergence for the inclusive case and for the prediction with a jet veto upon the inclusion of the NNLO QCD corrections.

DOI: 10.1103/PhysRevD.106.074016

I. INTRODUCTION

Studying vector boson production in association with multijet final states at the Large Hadron Collider (LHC) offers a wide variety of interesting phenomenological explorations. In particular, the production of a W boson in association with bottom quark (b) jets is very interesting both from experimental and theoretical perspectives. It is crucial to scrutinize experimental signatures for both $\mathrm{W} + 1b$ jet and $\mathrm{W} + 2b$ jets, in order to test our knowledge of the strong interaction at high energies and improve our modeling of bottom-quark jets at the LHC. The cross sections for both the signatures have been measured at the Tevatron [1,2] and LHC [3–6]. While the $\mathrm{W} + 1b$ jet signature provides a fundamental probe of the bottom-quark parton distribution functions (PDFs), the $\mathrm{W} + 2b$ jets final state constitutes an irreducible background to many important reactions studied at the LHC, such as the Higgs-strahlung process [$\mathrm{pp} \to \mathrm{WH}$ ($\mathrm{H} \to b\bar{b}$)] and single top production [$\mathrm{pp} \to \bar{b}t$ ($t \to \mathrm{W}b$)], as well as many beyond the Standard Model (BSM) searches. Moreover, the $\mathrm{W} + b$ jets processes are interesting from a theoretical point of view as they are a perfect testing ground to study the different ways of treating the b quark. In particular, the choice of whether to take its mass and presence in the PDF into account leads to two disparate computational schemes: the four- (4FS) and five-flavor number schemes (5FS).

In this paper, we compute the NNLO QCD corrections to W boson production in association with a bottom-quark pair, which we henceforth call W$b\bar{b}$, including the leptonic decay of the W boson ($\mathrm{W} \to \ell\nu$). We work in 5FS, thus treating the bottom quark, and additionally the charged leptons, as massless particles. They contribute to the $\mathrm{W} + 2b$ jets signature, as well as $\mathrm{W} + 1b$ jet production when at least one b jet is tagged. Extensive studies of W$b\bar{b}$ production at NLO QCD accuracy [7–12] indicate a poor perturbative behavior at such order (i.e., the corrections are large, and the scale uncertainties do not improve with respect to the leading order predictions for inclusive final state) due to the opening of the qg-initiated channel. Several efforts to assess corrections beyond NLO were done by including additional jet radiations [13,14]. It is clear that a fully fledged NNLO QCD prediction is mandatory to improve the perturbative convergence of W$b\bar{b}$ production.

Improvement of theoretical precision is also a critical component of the progress in particle physics, as we enter the precision LHC era with the upcoming Run 3 and high-luminosity phases. We have seen spectacular breakthroughs in perturbative QCD calculations in the recent years, with a number of $2 \to 3$ processes computed at NNLO QCD accuracy for fully massless final states [15–20].

*hbhartanto@hep.phy.cam.ac.uk
†poncelet@hep.phy.cam.ac.uk
‡popescu@hep.phy.cam.ac.uk
§simone.zoia@unito.it

This success stems from both the advancements in the scattering amplitude computations and the developments of NNLO subtraction schemes.

The analytic computation of the required two-loop five-particle amplitudes is one of the main bottlenecks toward achieving NNLO QCD accuracy for $2 \to 3$ processes. However, the progress for five-particle processes with a single massive external particle has been spectacular recently. All planar two-loop five-particle Feynman integrals are now available analytically [21–24] in terms of bases of special functions, which substantially simplify computation of the finite remainders and allow for an extremely efficient numerical evaluation [25,26]. Partial results for the nonplanar integral families have also become available recently [27–29]. This progress resulted in a number of two-loop amplitudes computed at leading color [25,30–32]. In this work, we derive the analytic form of the leading color two-loop amplitude contributing to $\mathrm{W}(\to \ell\nu) b\bar{b}$ production and employ it to compute a number of observables for this process at NNLO in QCD. Our computation marks a significant precision-calculation milestone, since it represents the very first prediction to be derived for a $2 \to 3$ process involving a massive final state.

This paper is structured as follows. We begin by discussing the derivation of the required two-loop matrix elements and the tools used to perform the cross section computation and then present phenomenological results for the cross section and a number of interesting differential distributions.

II. CALCULATION

We consider $\mathrm{pp} \to \mathrm{W}^+(\to \ell^+\nu) b\bar{b}$ production (with $\ell = e$ or μ) up to $\mathcal{O}(\alpha^2\alpha_s^4)$. The calculation has been performed within the STRIPPER framework, a C++ implementation of the four-dimensional formulation of the sector-improved residue subtraction scheme [33–35]. The tree-level matrix elements are supplied by the AVH library [36], while the one-loop matrix elements are provided by the OpenLoops package [37,38]. We compute the double virtual contribution $\mathcal{V}^{(2)}$ in the leading color approximation for

$$u(p_1) + \bar{d}(p_2) \to b(p_3) + \bar{b}(p_4) + \ell^+(p_5) + \nu(p_6). \quad (1)$$

It consists of the (color and helicity summed) two-loop and one-loop squared matrix elements,

$$\mathcal{V}^{(2)} = \sum_{\text{col.}} \sum_{\text{hel.}} \{2\mathrm{Re}[M^{(0)*}\mathcal{F}^{(2)}] + |\mathcal{F}^{(1)}|^2\}, \quad (2)$$

where $M^{(0)}$ is the tree-level amplitude, and $\mathcal{F}^{(L)}$ is the L-loop finite remainder. We decompose $\mathcal{V}^{(2)}$ at leading color into

$$\mathcal{V}^{(2)}_{\mathrm{LC}} = \mathcal{V}^{(2),1} + \frac{n_f}{N_c}\mathcal{V}^{(2),n_f} + \frac{n_f^2}{N_c^2}\mathcal{V}^{(2),n_f^2}, \quad (3)$$

where n_f is the number of massless closed fermion loops. We note that the leading-color approximation is only enforced in the scale-independent part of the double virtual contribution,

$$\mathcal{V}^{(2)}(\mu_R^2) = \mathcal{V}^{(2)}_{\mathrm{LC}}(s_{12}) + \sum_{i=1}^{4} c_i \ln^i\left(\frac{\mu_R^2}{s_{12}}\right), \quad (4)$$

where $s_{ij} = (p_i + p_j)^2$ [p_i is the partonic momentum defined in Eq. (1)], μ_R is the renormalization scale, and the kinematic-dependent coefficients c_i are expressed in terms of full color lower-order matrix elements.[1]

The analytic computation of the two-loop amplitude follows closely Ref. [25], with modifications implemented to incorporate the decay of the W boson. We note that the inclusion of the W-boson decay increases the complexity of the calculation substantially with respect to the one with an on-shell W, carried out in Ref. [25]. Since the QCD corrections do not apply to the $\mathrm{W} \to \ell\nu$ decay, we can separate the six-point squared amplitude $\mathcal{M}_6^{(2)}$ into the product of the five-point W-production squared amplitude $\mathcal{M}_{5\mu\nu}^{(2)}$ and the leptonic tensor $\mathcal{D}^{\mu\nu}$,

$$\mathcal{M}_6^{(2)} = \mathcal{M}_{5\mu\nu}^{(2)}\mathcal{D}^{\mu\nu}|P(s_{56})|^2, \quad (5)$$

where $P(s) = 1/(s - M_W^2 + iM_W\Gamma_W)$ is the W-boson propagator factor. We perform tensor decomposition on the five-point W-production squared amplitude,

$$\mathcal{M}_5^{(2)\mu\nu} = \sum_{i=1}^{16} a_i^{(2)} v_i^{\mu\nu}, \quad (6)$$

using $\{p_1, p_2, p_3, p_5 + p_6\}$ as the spanning basis to build the $v_i^{\mu\nu}$ basis tensors [39,40]. The coefficients $a_i^{(2)}$ can be determined by contracting Eq. (6) with $v_{i\mu\nu}$ and inverting the resulting linear system of equations. The analytic form of the *contracted* squared amplitudes $v_{i\mu\nu}\mathcal{M}_5^{(2)\mu\nu}$ was derived using

[1]We chose this decomposition because in the STRIPPER scheme, all logarithms of the renormalization (and factorization) scale are kept explicitly. Only those up to power 2 are contributing to cross sections and the higher powers cancel. This cancellation is done numerically within STRIPPER scheme and serves as a cross check. To ensure this cancellation, we keep the logarithmic coefficients of the two-loop contribution in full color and consequently, evaluate the finite remainder at the scale s_{12}, such that the logarithmic terms in Eq. (4) match exactly those coming from the real radiation. However, we checked explicitly that using a different scale, such as H_T (7), leads to effects of $\mathcal{O}(1\%)$ at the cross section level, which are contained within the quoted scale uncertainties.

finite-field reconstruction methods within the FINITEFLOW framework [41,42]. We expressed them in terms of the special functions of Ref. [26] and rational coefficients, which we simplified using MULTIVARIATEAPART [43] and SINGULAR [44]. We further implemented these amplitudes in C++ for a fast numerical evaluation. We evaluate the special functions using the PENTAGONFUNCTIONS++ library [26]. Our analytic result is validated numerically against the $\mathrm{W}+4$ quarks helicity amplitudes derived in Ref. [31] at the level of the helicity-summed squared finite remainder, obtained after renormalization and subtraction of IR singularities. We note that our calculation employs significantly different methodologies with respect to Ref. [31]. We work with squared matrix elements and carried out the calculation in the CDR scheme employing the Larin prescription for the treatment of γ_5, while Ref. [31] derives the helicity amplitudes in the t'Hooft-Veltman scheme. The agreement between the two independent calculations not only provides a strong and nontrivial cross check, but it is also important to practically demonstrate the consistency of different schemes, particularly in treating the γ_5. The complete analytic expression is included in Supplemental Material [45].

III. PHENOMENOLOGY

We present numerical results for the LHC center-of-mass energy $\sqrt{s} = 8$ TeV, focusing on the $\mathrm{W}^+(\to \ell^+\nu) b\bar{b}$ final state. The Standard Model input parameters are

$$M_W = 80.351972 \text{ GeV}, \qquad \Gamma_W = 2.0842989 \text{ GeV},$$
$$M_Z = 91.153481 \text{ GeV}, \qquad \Gamma_Z = 2.4942665 \text{ GeV},$$
$$G_F = 1.16638 \times 10^{-5} \text{ GeV}^{-2},$$

from which the electromagnetic coupling α can be derived within the G_μ scheme. We assume a diagonal CKM matrix and employ the `=NNPDF31_as_0118= PDF sets` [46] with its perturbative order matching that of the corresponding calculations. Since we treat the bottom quark as massless, we need a flavor-sensitive jet algorithm to define the flavored jets in an infrared-safe way. The partons are clustered into a jet using the flavor-k_T jet algorithm [47] with $R = 0.5$. The jets (including b jets) and charged leptons are required to fulfill the following event-selection criteria [6]:

$$p_{\mathrm{T},\ell} > 30 \text{ GeV}, \qquad |\eta_\ell| < 2.1,$$
$$p_{\mathrm{T},j} > 25 \text{ GeV}, \qquad |\eta_j| < 2.4.$$

The central values of renormalization and factorization scales are set to be equal, $\mu_R = \mu_F = H_\mathrm{T}$, with

$$H_\mathrm{T} = E_\mathrm{T}(\ell\nu) + p_\mathrm{T}(b_1) + p_\mathrm{T}(b_2), \tag{7}$$

where b_1, b_2 are correspondingly the hardest and second hardest b-flavored (either b or $\bar{b}$) jets. $E_\mathrm{T}(\ell\nu) = \sqrt{M^2(\ell\nu) + p_\mathrm{T}^2(\ell\nu)}$ is the transverse energy of the off-shell W boson, with $M(\ell\nu)$ and $p_\mathrm{T}(\ell\nu)$ being its invariant mass and transverse momentum, respectively. Unless otherwise specified, the scale uncertainties are obtained using the seven-point scale variation, where μ_R and μ_F are varied by a factor of 2 around H_T, while satisfying the $1/2 \le \mu_R/\mu_F \le 2$ constraint.

Based on the number of jets required in the final states, we can define the following configurations for the NLO and NNLO predictions:

(i) inclusive (inc): at least $2b$ jets;
(ii) exclusive (exc): exactly $2b$ jets and no other jets.

The naïve scale variation of the exclusive prediction generally leads to an underestimation of the scale uncertainties [48]. For processes with a large $\mathcal{K}$ factor, however, the standard scale variation prescription may be insufficient to capture the missing higher-order effects also in the inclusive calculation. This indeed applies to the $Wb\bar{b}$ process under consideration. Hence, for the exclusive configuration, we use also the uncorrelated prescription of Ref. [48], in addition to the seven-point scale variation. To obtain the uncorrelated scale uncertainty, we first write the exlusive cross section as follows (we use the NNLO case as an example):

$$\sigma_\mathrm{NNLO,exc} = \sigma_\mathrm{NNLO,inc} - \sigma_\mathrm{NLO+1}{}_{j\mathrm{,inc}}, \tag{8}$$

where $\sigma_\mathrm{NNLO,exc}$ ($\sigma_\mathrm{NNLO,inc}$) is the NNLO $Wb\bar{b}$ exclusive (inclusive) cross section, while $\sigma_{\mathrm{NLO+1}j\mathrm{,inc}}$ is the $Wb\bar{b}j$ inclusive NLO cross section. The jet-veto value follows the jet definition specified above. The uncorrelated scale uncertainty is then obtained by adding the individually scale-varied cross sections in quadrature

$$\Delta\sigma_\mathrm{NNLO,exc} = \sqrt{(\Delta\sigma_\mathrm{NNLO,inc})^2 + (\Delta\sigma_{\mathrm{NLO+1}j\mathrm{,inc}})^2}, \tag{9}$$

where $\Delta\sigma_\mathrm{NNLO,inc}$ ($\Delta\sigma_{\mathrm{NLO+1}j\mathrm{,inc}}$) is the scale uncertainty of the inclusive NNLO $\mathrm{W}b\bar{b}$ (NLO $\mathrm{W}b\bar{b}j$) cross section computed using the standard seven-point scale variation.

In Table I, we present numerical results for the fiducial cross section for the inclusive and exclusive configurations at different perturbative orders. As observed in the previous studies [9,14], the NLO QCD corrections are large in the case of the inclusive phase space. In our calculation, this amounts to about 70% corrections. The jet veto in the exclusive selection reduces the NLO QCD corrections to a moderate 17%. A similar observation holds at NNLO QCD, where we find a positive correction of 23% in the inclusive and 6.7% in the exclusive case. The NNLO QCD corrections are smaller than the NLO QCD corrections in both cases indicating perturbative convergence. In that respect, by using the scale dependence as the canonical way to estimate the uncertainties from missing higher orders, we conclude that theoretical uncertainty reduces with inclusion of higher order terms. However, for the

TABLE I. Fiducial cross sections for $pp \to W^+(\to \ell^+\nu) b\bar{b}$ production at the LHC with $\sqrt{s} = 8$ TeV at LO, NLO and NNLO for both inclusive (inc) and exclusive (exc) final states. The corresponding NNLO and NLO $\mathcal{K}$ factors are defined as $\mathcal{K}_{\rm NNLO} = \sigma_{\rm NNLO}/\sigma_{\rm NLO}$ and $\mathcal{K}_{\rm NLO} = \sigma_{\rm NLO}/\sigma_{\rm LO}$. The statistical errors are shown for the central predictions. Scale uncertainties for the exclusive predictions are provided using both the standard seven-point scale variation and uncorrelated prescription of Ref. [48]. The latter is quoted inside parentheses in the error estimates.

	Inclusive [fb]	$\mathcal{K}_{\rm inc}$	Exclusive [fb]	$\mathcal{K}_{\rm exc}$
$\sigma_{\rm LO}$	$213.2(1)^{+21.4\%}_{-16.1\%}$	⋯	$213.2(1)^{+21.4\%}_{-16.1\%}$	⋯
$\sigma_{\rm NLO}$	$362.0(6)^{+13.7\%}_{-11.4\%}$	1.7	$249.8(4)^{+3.9(+41)\%}_{-6.0(-28)\%}$	1.17
$\sigma_{\rm NNLO}$	$445(5)^{+6.7\%}_{-7.0\%}$	1.23	$267(3)^{+1.8(+16)\%}_{-2.5(-16)\%}$	1.067

inclusive phase space, the NLO corrections are significantly larger than the LO scale dependence. The situation at NNLO QCD slightly improves, but the corrections are still only barely covered by the NLO scale band. For the exclusive case, the NLO corrections are within the LO band; however, the estimated uncertainty from the seven-point scale variation is comparatively small, only 5%. The NNLO corrections here are also smaller but are well outside the NLO scale uncertainty, indicating that the NLO scale dependence is underestimated. This motivates the alternative prescription of Ref. [48] to estimate theory uncertainties, taking into account the jet veto effect. The uncertainties resulting from this prescription are shown in the parentheses and are significantly larger. The higher-order corrections fall well within the uncertainty bands, implying that this method is more reliable, but also quite conservative.

The double virtual corrections, which have been included only in the leading color approximation, deserve an additional comment. For the inclusive setup, we find that the contribution of Eq. (4) to the cross section is about 5%. In the exclusive case, the Born configurations are unaffected by the jet veto, but a fraction of the hard radiative corrections are suppressed. This leads to an enhancement of the sensitivity to the double virtual matrix element, which contributes ∼10% of the fiducial cross section in this case. The naïve expectation for the subleading color effects is that they are about 10% of the double virtual matrix element, implying that potential corrections to the fiducial cross section would be about 1% (0.5%) for the exclusive (inclusive) case.

Turning to the differential distributions, we present the transverse momentum of the charged lepton, $p_{\mathrm{T},\ell}$, in Fig. 1, for the inclusive, as well as exclusive, phase space selection. Focusing on the perturbative convergence of the spectrum, we can draw similar conclusions as for the fiducial cross section. In the inclusive case, we find sizeable NNLO QCD corrections of ∼20%, which are barely

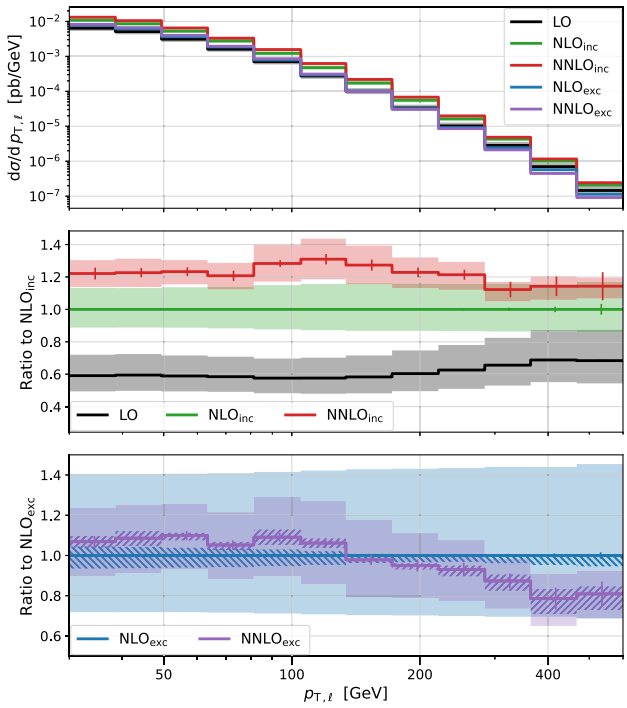

FIG. 1. The charged lepton's transverse momentum distribution. The upper panel shows the absolute predictions for the inclusive and exclusive selection at different perturbative orders. The middle panel shows the inclusive cross sections as a ratio with respect to the central NLO prediction, with the colored bands indicating the seven-point scale variation. The lower panel shows the same ratio for the exclusive configuration. Here, the colored bands correspond to the decorrelated scale variation, and the hashed bands to the standard 7-point variation. The vertical bars indicate the statistical uncertainty.

contained in the NLO uncertainty. The corrections have a tendency to increase at higher energies, being the largest around $p_{\mathrm{T},\ell} \approx 100$ GeV, similarly to the NLO corrections. For the exclusive phase space, we find positive corrections of about 7% for low $p_{\mathrm{T},\ell}$, and negative corrections of order ∼10% for $p_{\mathrm{T},\ell} > 100$ GeV. Again, we observe that the decorrelated prescription to estimate the uncertainty is more reliable.

The next two distributions characterize the $b\bar{b}$ system. In Fig. 2, we show the transverse momentum of the $b\bar{b}$ system, $p_{\mathrm{T},b\bar{b}}$. In terms of perturbative corrections, we find a similar trend as for the charged lepton transverse momentum. Additionally, the absolute distributions highlight that the inclusive spectrum is, in general, harder than the exclusive case, confirming the intuition that the jet veto suppresses additional large transverse momentum jets. In the case of exclusive phase space, this differential distribution can be understood as a proxy for the W transverse momentum.

The distribution of the invariant mass of the $b\bar{b}$ system, $M_{b\bar{b}}$, is shown in Fig. 3. This observable is interesting when considering the QCD process $Wb\bar{b}$ as background to the

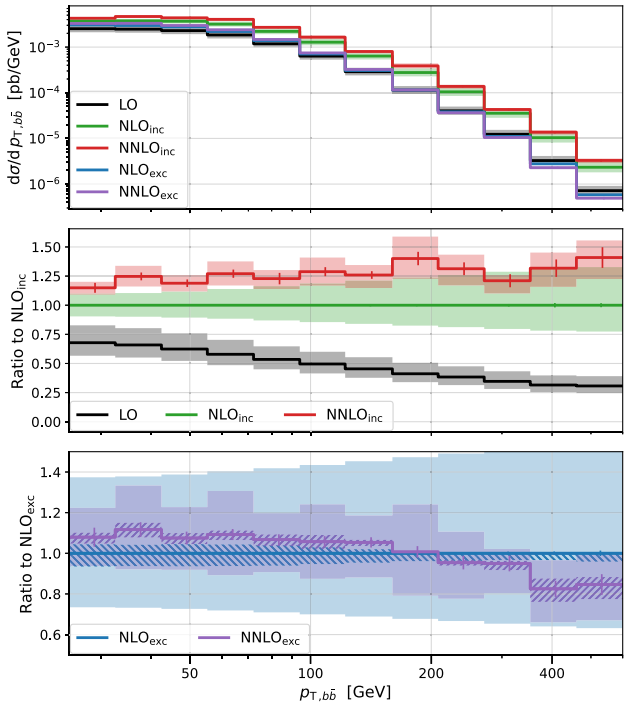

FIG. 2. Transverse momentum distribution of the $b\bar{b}$ system. Same layout as in Fig. 1.

Higgs-strahlung process WH($\to b\bar{b}$). Around the Higgs mass, we can see that the NNLO QCD corrections are about 20% in the inclusive selection and only ∼5% in the exclusive case. By comparing the two prescriptions for estimating the uncertainty, we see that around the Higgs mass, the seven-point prescription implies a two to three times smaller uncertainty than the decorrelated method.

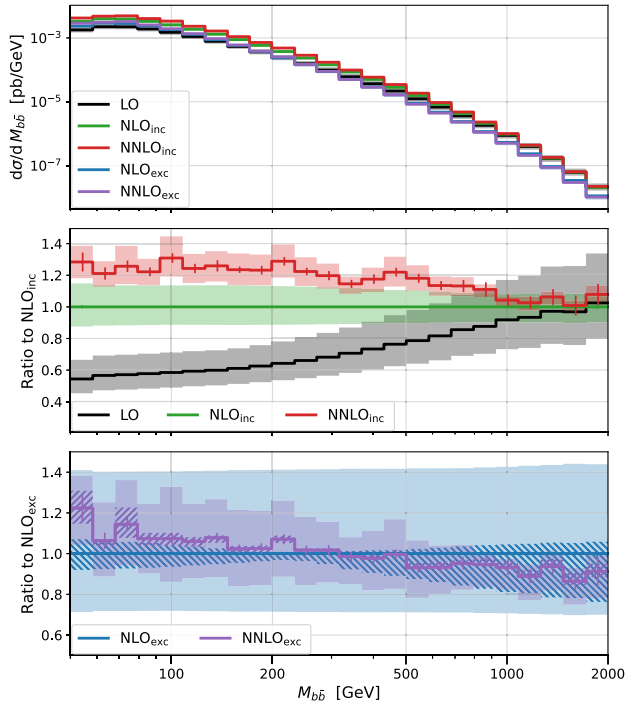

FIG. 3. Invariant mass distribution of the $b\bar{b}$ system. Same layout as in Fig. 1.

Finally, we would like to comment on the fluctuations between bins in the presented differential observables. We checked that these fluctuations are indeed compatible with those expected from Monte Carlo integration to exclude numerical instabilities as their source. The contributions from double real radiation diagrams have the largest statistical uncertainty and also required the largest computational effort. The reader is invited to find our results for other observables in Supplemental Material [45] to this publication.

IV. CONCLUSIONS

We presented fiducial and differential cross sections for the $Wb\bar{b}$ process at the LHC with 8 TeV center-of-mass energy. This includes the computation of the double virtual amplitudes in the leading color approximation with incorporated decay of the W boson.

We addressed the observation of large NLO QCD corrections in this process and found that the NNLO QCD corrections are significantly smaller. We observe a significant reduction of the scale dependence, which indicates perturbative convergence. We discussed the behavior of the jet-vetoed cross section, which exhibits much smaller corrections but suffers from accidental cancellations in the scale dependence, rendering the theory uncertainty estimates from canonical scale variation unreliable. At NNLO accuracy, we validated the alternative prescription of Ref. [48] for estimating the theory uncertainties.

This work constitutes the first NNLO QCD calculation for a $2 \to 3$ process including a massive final state particle. Studying this class of processes at such accuracy is of the utmost importance for the physics programme of the LHC. However, the steep requirements for amplitudes involving many loops and high multiplicities used to put them beyond the reach of computational capabilities. Our results demonstrate that the door of precision phenomenology is finally open for these processes as well.

ACKNOWLEDGMENTS

The authors would like to thank Michał Czakon for making the STRIPPER library available to us, Vasily Sotnikov for help in the comparison with the results of Ref. [31], and Simon Badger and Alexander Mitov for many inspiring discussions and useful comments on the draft. This project received funding from the European Union's Horizon 2020 research and innovation programmes *New level of theoretical precision for LHC Run 2 and beyond* (Grant No. 683211), and *High precision multijet dynamics at the LHC* (Grant No. 772099). H. B. H. was partially supported by STFC consolidated HEP theory

Grant No. ST/T000694/1. S. Z. gratefully acknowledges the computing resources provided by the Max Planck Institute for Physics and by the Max Planck Computing & Data Facility. A. P. is also supported by the Cambridge Trust and Trinity College Cambridge. R. P. acknowledges the support from the Leverhulme Trust and the Isaac Newton Trust, as well as the use of the DiRAC Cumulus HPC facility under Grant No. PPSP226. The DiRAC component of CSD3 was funded by BEIS capital funding via STFC capital Grants No. ST/P002307/1 and No. ST/R002452/1 and STFC operations Grant No. ST/R00689X/1.

[1] V. M. Abazov *et al.* (D0 Collaboration), A Search for $Wb\bar{b}$ and WH Production in $p\bar{p}$ Collisions at $\sqrt{s} = 1.96$ TeV, Phys. Rev. Lett. **94**, 091802 (2005).
[2] V. M. Abazov *et al.* (D0 Collaboration), Measurement of the $p\bar{p} \to W + b + X$ production cross section at $\sqrt{s} =$ 1.96 TeV, Phys. Lett. B **718**, 1314 (2013).
[3] G. Aad *et al.* (ATLAS Collaboration), Measurement of the cross section for the production of a W boson in association with b^- jets in pp collisions at $\sqrt{s} = 7$ TeV with the ATLAS detector, Phys. Lett. B **707**, 418 (2012).
[4] G. Aad *et al.* (ATLAS Collaboration), Measurement of the cross-section for W boson production in association with b-jets in pp collisions at $\sqrt{s} = 7$ TeV with the ATLAS detector, J. High Energy Phys. 06 (2013) 084.
[5] S. Chatrchyan *et al.* (CMS Collaboration), Measurement of the production cross section for a W boson and two b jets in pp collisions at $\sqrt{s} = 7$ TeV, Phys. Lett. B **735**, 204 (2014).
[6] V. Khachatryan *et al.* (CMS Collaboration), Measurement of the production cross section of a W boson in association with two b jets in pp collisions at $\sqrt{s} = 8$ TeV, Eur. Phys. J. C **77**, 92 (2017).
[7] R. K. Ellis and S. Veseli, Strong radiative corrections to W b anti-b production in p anti-p collisions, Phys. Rev. D **60**, 011501 (1999).
[8] F. Febres Cordero, L. Reina, and D. Wackeroth, NLO QCD corrections to W boson production with a massive b-quark jet pair at the Tevatron p anti-p collider, Phys. Rev. D **74**, 034007 (2006).
[9] F. Febres Cordero, L. Reina, and D. Wackeroth, W- and Z-boson production with a massive bottom-quark pair at the Large Hadron Collider, Phys. Rev. D **80**, 034015 (2009).
[10] S. Badger, J. M. Campbell, and R. K. Ellis, QCD corrections to the hadronic production of a heavy quark pair and a W boson including decay correlations, J. High Energy Phys. 03 (2011) 027.
[11] C. Oleari and L. Reina, $W^{\pm}b\bar{b}$ production in POWHEG, J. High Energy Phys. 08 (2011) 061; Erratum, 11 (2011) 40.
[12] R. Frederix, S. Frixione, V. Hirschi, F. Maltoni, R. Pittau, and P. Torrielli, W and $Z/\gamma*$ boson production in association with a bottom-antibottom pair, J. High Energy Phys. 09 (2011) 061.
[13] G. Luisoni, C. Oleari, and F. Tramontano, $Wb\bar{b}j$ production at NLO with POWHEG + MiNLO, J. High Energy Phys. 04 (2015) 161.
[14] F. R. Anger, F. Febres Cordero, H. Ita, and V. Sotnikov, NLO QCD predictions for $Wb\bar{b}$ production in association with up to three light jets at the LHC, Phys. Rev. D **97**, 036018 (2018).
[15] H. A. Chawdhry, M. L. Czakon, A. Mitov, and R. Poncelet, NNLO QCD corrections to three-photon production at the LHC, J. High Energy Phys. 02 (2020) 057.
[16] S. Kallweit, V. Sotnikov, and M. Wiesemann, Triphoton production at hadron colliders in NNLO QCD, Phys. Lett. B **812**, 136013 (2021).
[17] H. A. Chawdhry, M. Czakon, A. Mitov, and R. Poncelet, NNLO QCD corrections to diphoton production with an additional jet at the LHC, J. High Energy Phys. 09 (2021) 093.
[18] M. Czakon, A. Mitov, and R. Poncelet, Next-to-Next-to-Leading Order Study of Three-Jet Production at the LHC, Phys. Rev. Lett. **127**, 152001 (2021).
[19] S. Badger, T. Gehrmann, M. Marcoli, and R. Moodie, Next-to-leading order QCD corrections to diphoton-plus-jet production through gluon fusion at the LHC, Phys. Lett. B **824**, 136802 (2022).
[20] X. Chen, T. Gehrmann, N. Glover, A. Huss, and M. Marcoli, Automation of antenna subtraction in color space: Gluonic processes, arXiv:2203.13531.
[21] C. G. Papadopoulos, D. Tommasini, and C. Wever, The pentabox master integrals with the simplified differential equations approach, J. High Energy Phys. 04 (2016) 078.
[22] S. Abreu, H. Ita, F. Moriello, B. Page, W. Tschernow, and M. Zeng, Two-loop integrals for planar five-point one-mass processes, J. High Energy Phys. 11 (2020) 117.
[23] D. D. Canko, C. G. Papadopoulos, and N. Syrrakos, Analytic representation of all planar two-loop five-point master integrals with one off-shell leg, J. High Energy Phys. 01 (2021) 199.
[24] N. Syrrakos, Pentagon integrals to arbitrary order in the dimensional regulator, J. High Energy Phys. 06 (2021) 037.
[25] S. Badger, H. B. Hartanto, and S. Zoia, Two-Loop QCD Corrections to $Wb\bar{b}$ Production at Hadron Colliders, Phys. Rev. Lett. **127**, 012001 (2021).
[26] D. Chicherin, V. Sotnikov, and S. Zoia, Pentagon functions for one-mass planar scattering amplitudes, J. High Energy Phys. 01 (2022) 096.
[27] C. G. Papadopoulos and C. Wever, Internal reduction method for computing Feynman integrals, J. High Energy Phys. 02 (2020) 112.
[28] S. Abreu, H. Ita, B. Page, and W. Tschernow, Two-loop hexa-box integrals for nonplanar five-point one-mass processes, J. High Energy Phys. 03 (2022) 182.

[29] A. Kardos, C. G. Papadopoulos, A. V. Smirnov, N. Syrrakos, and C. Wever, Two-loop nonplanar hexa-box integrals with one massive leg, J. High Energy Phys. 05 (2022) 033.
[30] S. Badger, H. B. Hartanto, J. Kryś, and S. Zoia, Two-loop leading-color QCD helicity amplitudes for Higgs boson production in association with a bottom-quark pair at the LHC, J. High Energy Phys. 11 (2021) 012.
[31] S. Abreu, F. Febres Cordero, H. Ita, M. Klinkert, B. Page, and V. Sotnikov, Leading-color two-loop amplitudes for four partons and a W boson in QCD, J. High Energy Phys. 04 (2022) 042.
[32] S. Badger, H. B. Hartanto, J. Kryś, and S. Zoia, Two-loop leading color helicity amplitudes for $W^{\pm}\gamma + j$ production at the LHC, J. High Energy Phys. 05 (2022) 035.
[33] M. Czakon, A novel subtraction scheme for double-real radiation at NNLO, Phys. Lett. B **693**, 259 (2010).
[34] M. Czakon and D. Heymes, Four-dimensional formulation of the sector-improved residue subtraction scheme, Nucl. Phys. **B890**, 152 (2014).
[35] M. Czakon, A. van Hameren, A. Mitov, and R. Poncelet, Single-jet inclusive rates with exact color at $\mathcal{O}(\alpha_s^4)$, J. High Energy Phys. 10 (2019) 262.
[36] M. Bury and A. van Hameren, Numerical evaluation of multi-gluon amplitudes for High Energy Factorization, Comput. Phys. Commun. **196**, 592 (2015).
[37] F. Buccioni, S. Pozzorini, and M. Zoller, On-the-fly reduction of open loops, Eur. Phys. J. C **78**, 70 (2018).
[38] F. Buccioni, J.-N. Lang, J. M. Lindert, P. Maierhöfer, S. Pozzorini, H. Zhang, and M. F. Zoller, OpenLoops 2, Eur. Phys. J. C **79**, 866 (2019).
[39] L. Chen, A prescription for projectors to compute helicity amplitudes in D dimensions, Eur. Phys. J. C **81**, 417 (2021).
[40] T. Peraro and L. Tancredi, Tensor decomposition for bosonic and fermionic scattering amplitudes, Phys. Rev. D **103**, 054042 (2021).
[41] T. Peraro, Scattering amplitudes over finite fields and multivariate functional reconstruction, J. High Energy Phys. 12 (2016) 030.
[42] T. Peraro, FiniteFlow: Multivariate functional reconstruction using finite fields and dataflow graphs, J. High Energy Phys. 07 (2019) 031.
[43] M. Heller and A. von Manteuffel, MultivariateApart: Generalized partial fractions, Comput. Phys. Commun. **271**, 108174 (2022).
[44] W. Decker, G.-M. Greuel, G. Pfister, and H. Schönemann, Singular 4-2-1—A computer algebra system for polynomial computations, http://www.singular.uni-kl.de (2021).
[45] See Supplemental Material at http://link.aps.org/supplemental/10.1103/PhysRevD.106.074016 for complete analytic expression.
[46] R. D. Ball *et al.* (NNPDF Collaboration), Parton distributions from high-precision collider data, Eur. Phys. J. C **77**, 663 (2017).
[47] A. Banfi, G. P. Salam, and G. Zanderighi, Infrared safe definition of jet flavor, Eur. Phys. J. C **47**, 113 (2006).
[48] I. W. Stewart and F. J. Tackmann, Theory uncertainties for Higgs and other searches using jet bins, Phys. Rev. D **85**, 034011 (2012).